Contribution No. 2043 from the Central Research Department,
E. I. du Pont de Nemours and Company, Wilmington, Delaware 19898

Crystal Structure and Stereochemical Nonrigidity of $TaH(CO)_2[(CH_3)_2PCH_2CH_2P(CH_3)_2]_2$

P. MEAKIN,* L. J. GUGGENBERGER,* F. N. TEBBE, and J. P. JESSON

Received June 23, 1973 AIC30767Z

The crystal structure of $TaH(CO)_2[(CH_3)_2PCH_2CH_2P(CH_3)_2]_2$ has been determined from room-temperature X-ray diffractometer data. The tantalum atom is seven coordinate and bonded to two chelated diphosphine ligands, two carbonyl ligands, and a hydride ligand. The coordination polyhedron is that of a distorted capped octahedron where the hydride hydrogen is the capping ligand. The Ta–P distance is 2.514 (16) Å and the P–Ta–P angle for the chelated diphosphine is 75.8 (3)°. The diphosphine ligand stereochemistry is disordered with preferred conformations similar to those frequently observed in chelated diphosphine transition metal complexes. The temperature-dependent hydride region ^1H nmr spectra and ^{31}P nmr spectra (with and without ^1H noise decoupling) have been recorded in both the continuous wave and Fourier modes over the temperature range −10 to 100°. The low-temperature limit proton noise decoupled ^{31}P nmr spectrum in solution can be accurately fitted using an AA'BB' model. This observation is consistent with the solution structure being the same as the crystal structure. An analysis of the temperature-dependent line shapes for the hydride region ^1H nmr spectra in solution at 90 and 220 MHz indicates that the exchange process must involve an equilibrium with a second isomer present in low concentrations. The free energy of activation for the "mutual" exchange process is estimated to be 12.8 kcal mol^{-1} at 27°. Crystals are monoclinic, space group $P2_1/c$, with cell dimensions of $a = 8.963$ (5), $b = 12.467$ (4), $c = 12.552$ (5) Å, and $\beta = 125.53$ (6)°. The observed and calculated densities for two molecules per cell are 1.55 and 1.57 g/cm^3, respectively. The structure was refined by least squares to a conventional R of 0.13 for 935 observed reflections.

Introduction

We have previously investigated stereochemical nonrigidity in a series of hydrides of the form H_nML_4 for the cases of five,[1,2] six,[3,4] and eight coordination[5,6] (M is a transition metal and L a trivalent phosphorus ligand). In the present paper we describe an X-ray and nmr study of the stereochemistry and stereochemical nonrigidity of the seven-coordinate hydride $TaH(CO)_2[(CH_3)_2PCH_2CH_2P(CH_3)_2]_2$. Although it does not fit the general formula for the hydrides studied previously, we believe it to be the first seven-coordinate system examined in detail in terms of its exchange behavior in the nmr and that the types of motion involved in the rearrangement can be meaningfully compared with those we have considered in the H_nML_4 series. A combination of X-ray and nmr studies is desirable in studying stereochemical nonrigidity. The crystal structure establishes the preferred configuration for the solid state and can give some indication of the most probable transition state geometry for mutual exchange processes in solution. These processes are in turn conveniently studied by temperature-dependent nmr line shape changes. We have determined crystal structures in the H_nML_4 series for six[7,8] and eight coordination,[9] and examples of five coordination have been presented by other workers.[10]

Initially it appeared that it would be difficult to establish the molecular structure of $TaH(CO)_2[(CH_3)_2PCH_2CH_2P(CH_3)_2]_2$ by diffraction techniques since disorder was very strongly indicated. The space group required $C_i(\bar{1})$ molecular point symmetry which, of course, a bona fide seven-coordinate complex cannot have. There remained the intriguing possibility of finding a regular six-coordinate tantalum stereochemistry with the hydride hydrogen being stereochemically inactive in the solid state, as apparently happens in some five-coordinated $RhHP_4$ complexes.[10] In spite of the disorder, the X-ray results define the overall molecular stereochemistry clearly but with less accuracy than would be possible with a completely ordered structure. The results show that the hydride hydrogen *is* stereochemically active, the tantalum atom being seven coordinate with the hydride hydrogen acting as the capping ligand of a distorted capped octahedron. The low-temperature limit ^{31}P nmr spectra are consistent with the geometry established in the solid. The nmr studies suggest that there is a low concentration of a second isomer in equilibrium with the major species in solution. The free energy of activation for the "mutual" exchange process is 12.8 kcal at 27°.

Experimental Section

Preparation of $TaH(CO)_2[(CH_3)_2PCH_2CH_2P(CH_3)_2]_2$. This complex was prepared from the very reactive species $TaH_5[(CH_3)_2PCH_2CH_2P(CH_3)_2]_2$ in benzene at 80° under carbon monoxide pressure. Details are available elsewhere.[11]

Cell Data and X-Ray Data Collection. All crystal handling was done in a drybox; crystals were placed in capillaries for all X-ray work. Crystals are monoclinic with cell dimensions of $a = 8.963$ (5), $b = 12.467$ (4), $c = 12.552$ (5) Å, and $\beta = 125.53$ (6)°; these parameters resulted from the least-squares refinement of the angular positions of eight reflections measured on the diffractometer. The space group $P2_1/c$ is uniquely determined from systematic absences observed on Weissenberg and precession films; the noncentric space groups Pc and $P2/c$ were also considered in view of the disorder (*vida infra*). The observed and calculated densities for two molecules per cell are 1.55 and 1.57 g/cm^3, respectively.

The cell data for $P2_1/c$ require that each molecule have $C_i(\bar{1})$ point symmetry. However, a metal atom which is seven coordinate cannot have this point symmetry if all ligands are stereochemically active. The indication was that the molecules were disordered with the disorder operator generating a center of inversion at the tantalum atom. Evidence for disorder was provided by films which showed that reflections with $k + l = 2n + 1$ were very weak. These reflec-

(1) P. Meakin, J. P. Jesson, F. N. Tebbe, and E. L. Muetterties, *J. Amer. Chem. Soc.*, 93, 1797 (1971).
(2) P. Meakin, E. L. Muetterties, and J. P. Jesson, *J. Amer. Chem. Soc.*, 94, 5271 (1972).
(3) P. Meakin, E. L. Muetterties, F. N. Tebbe, and J. P. Jesson, *J. Amer. Chem. Soc.*, 93, 4701 (1971).
(4) P. Meakin, E. L. Muetterties, and J. P. Jesson, *J. Amer. Chem. Soc.*, 95, 75 (1973).
(5) J. P. Jesson, E. L. Muetterties, and P. Meakin, *J. Amer. Chem. Soc.*, 93, 5261 (1971).
(6) P. Meakin, L. J. Guggenberger, W. G. Peet, E. L. Muetterties, and J. P. Jesson, *J. Amer. Chem. Soc.*, 95, 1467 (1973).
(7) L. J. Guggenberger, D. D. Titus, M. T. Flood, R. E. Marsh, A. A. Orio, and H. B. Gray, *J. Amer. Chem. Soc.*, 94, 1135 (1972).
(8) L. J. Guggenberger, *Inorg. Chem.*, 12, 1317 (1973).
(9) L. J. Guggenberger, *Inorg. Chem.*, 12, 2295 (1973).
(10) R. W. Baker and P. Pauling, *Chem. Commun.*, 1495 (1969); (b) R. W. Baker, B. Ilmaier, P. J. Pauling, and R. S. Nyholm, *ibid.*, 1077 (1970).
(11) F. N. Tebbe, *J. Amer. Chem. Soc.*, 95, 5823 (1973).

tions have contributions from the ligand atoms alone; tantalum atoms contribute only to $k + l = 2n$ reflections.[12]

A somewhat irregular platelet-like crystal of dimensions 0.30 × 0.16 × 0.25 mm was used in the data collection. The crystal was mounted with the [1,0,−1] axis along the ϕ axis of a Picker four-circle automatic diffractometer. A total of 1139 reflections were measured out to a 2θ of 40° using Zr filtered Mo radiation (λ 0.7107); both $hk0$ and $\bar{h}k0$ data were measured and then averaged. The θ–2θ scan technique was used with a scan range of 2.75° (1°/min) plus the $K\alpha_1$–$K\alpha_2$ separation. Individual backgrounds of 15 sec were measured before and after each peak. No crystal decomposition was observed.

The usual Lorentz and polarization corrections were applied and also an absorption correction using the program ACACA.[13] The linear absorption coefficient for Mo Kα radiation is 53.7 cm^{-1}. The crystal was defined by six plane faces for the absorption correction. The maximum and minimum observed transmission factors were 0.438 and 0.197, respectively. The structure factor errors were estimated according to a scheme reported earlier.[14] Those reflections with $F_o < (F_o)$ were considered "unobserved" and given zero weight in the refinement.

The tantalum atom position was determined from the Patterson function. The phosphorus atoms were determined from an electron density map. The phosphorus atom positions, especially P(2), allow phasing of some of the $k + l = 2n + 1$ reflections and thus break the pseudosymmetry of the electron density function caused by the special position of the tantalum atom. All of the peaks in an electron density difference map at this point were extremely broad, suggestive of extensive ligand disordering. A serious effort was made to fit these broad peaks with ordered ligand models; the best $R(\Sigma||F_o| - |F_c||/\Sigma|F_o|)$ obtained with ordered ligand models was 0.35.

In order to establish the nature of the disorder in the phosphine ligands, general electron density difference maps were calculated parallel and perpendicular to the PTaP plane of the ligand. The broad peaks could be accounted for by allowing for "flipping" of diphosphines between two configurations (*vide infra*). The disorder was handled in terms of individual atoms rather than a group refinement because the individual atom refinement involves fewer assumptions and, if it works, gives more stereochemical data in the end. The approach was to pick one ligand configuration from the electron density maps and then include the corresponding "flipped" configuration mathematically in the structure factor calculation. Specifically, this was done by attaching an internal orthogonal molecular coordinate system with X in the Ta to P(1)–P(2)′ midpoint direction, Y in the P(1)–P(2)′ direction, and Z completing the orthogonal coordinate system (primed atoms are at $-X, -Y, -Z$, shown in Figure 3). The picked configuration was then rotated by $C_2(2)$ about X and mirrored across Y to superimpose the two "flipped" configurations. All the atoms in one configuration were refined isotropically. The refinements always converged but with some tendency to oscillate with respect to the isotropic thermal parameters of some of the carbon atoms. There are other ways in which the disorder can be built into the model; they vary in the specific details of how each phosphorus tetrahedron is rotated but agree with respect to the overall stereochemistry obtained. Several of these other phosphine models which were generally consistent with the very broad electron density peaks were also refined; they gave slightly higher R factors and stereochemical results in general agreement with those reported here.

The carbonyl and hydride ligands are also disordered. This was observed as very broad peaks in electron density difference maps calculated parallel to the PTaP plane. The maximum intensities are centered above and below the tantalum atom but they are very broad in the P(1)–P(2) direction, parallel to the ligand bite. These peaks are interpreted in terms of a superposition of axial and off-axial carbonyl groups. An electron density difference map with an axial carbonyl in the model gave two distinct carbonyl groups on either side of the axial one in the pseudomirror plane of the molecule. Specifically, this disorder was described in the model by putting one carbonyl in the axial position and a second in one of the off-axial positions, and a third was mathematically included in the other off-axial position by rotating $C_2(2)$ about the previously defined molecular axis X. The latter two carbonyls are at one-half the multiplicity of the axial carbonyl. Both the axial and one of the off-axial carbonyls could be refined isotropically. However, the close proximity of the axial and off-axial carbonyl carbon atoms appeared to influence the refinement of these atoms, so in the final refinements the carbon atoms of the carbonyl groups were fixed at 1.15 Å from the appropriate oxygen atom toward the tantalum atom. A physical description of the disordered model will be given in the Structure Description section.

An anisotropic thermal parameter was used for the Ta atom; isotropic thermal parameters were used for all other atoms. No hydrogen atoms were included in the model because of the disorder, but the resultant stereochemistry is indicative of where the hydride hydrogen atom must be. The final R values for 935 observed reflections are 0.13 for R and 0.13 for R_w, $[\Sigma w(|F_o| - |F_c|)^2/\Sigma w|F_o|^2]^{1/2}$. However, this is extremely misleading for a model with one heavy atom ordered and everything else badly disordered. For an honest appraisal of the refinement the data must be separated into $k + l = 2n$ reflections which have contributions from all atoms and $k + l = 2n + 1$ reflections which have contributions from all atoms except the Ta atom. The latter is a true indication of the nature of the refinement for the ligand atoms. This breakdown is as follows for the observed data with the number of reflections involved given in parentheses.

	$k + l = 2n$	$k + l = 2n + 1$
R	0.09 (516)	0.23 (419)
R_w	0.10	0.20

Although the R of 0.23 is high, it must be remembered that all atoms involved in that agreement factor are badly disordered, with isotropic thermal parameters only, and without the hydrogen atom contributions. Final electron density difference maps were surprisingly clean. At the end of the refinement the crystal was remounted and some of the worst fitting data were remeasured to be absolutely sure that observed structure factor differences reflected errors in the model and not some machine error.

Atom scattering factors for neutral atoms were used.[15] The tantalum atom was corrected for the real and imaginary part of the anomalous scattering effect.[16] The function $\Sigma w(|F_o| - |F_c|)^2$ was minimized in the least-squares program SFLS5.

Serious consideration was given to the possibility of the space group not being $P2_1/c$. If the $0k0$ absences for k odd were fortuitous the space group could be $P2/c$ or Pc. The Ta atom at $0^1/_4 1/_4$ in both of these space groups would contribute only to k even for $0k0$ reflections and to $k + l$ even for general reflections, consistent with the $k + l$ odd reflections being observed weak. An ordered molecular structure in $P2/c$ could be dismissed quickly since the location of the required crystallographic twofold axis would lead to a significant disordering of the P atoms which we know are basically ordered from the $P2_1/c$ refinement. In principle the molecular structure could be ordered in Pc. Extensive calculations were done in Pc starting with the Ta at $0^1/_4 1/_4$ and the P atoms in positions transformed from their positions in $P2_1/c$. Then sequential portions of one diphosphine at a time were placed in the model and the effects were observed in electron density difference maps calculated in sections parallel and perpendicular to the PTaP plane. We could slowly build up a model resembling the $P2_1/c$ model, but the "flipped" diphosphine conformations were always present. We concluded that the molecular structure was disordered in Pc in a similar fashion as in $P2_1/c$. It follows necessarily that it would be disordered in $P2/c$ also. Hence, we further concluded that the $0k0$ absences for k odd reflections were truly indicative of a 2_1 axis.

Several general comments can be made about the disorder at this point. Although the Ta atom dominates the scattering here, our refinement was sensitive to both how many "light" atoms we had in the model, which can be partially attributed to scaling effects, and more importantly to positions of the ligand atoms. For comparison purposes, the conventional R for the Ta atom only in the model was 0.55 ($B = 3.0$ Å^2 and not varied), while the R with the Ta and P atoms in the model was 0.40 (B of Ta varied). Also it is important to note that the disorder observed is chemically and structurally very reasonable. The energy required to alter or even "flip" the diphosphine ligands is not great. On a precision ball and stick model this is a very facile process. In a crystal we would expect such a chemical process might lead to dynamic or static disorder or a combination of both. Disorder in the H and CO ligands follows naturally from that of the diphosphines.

(12) "International Tables for X-ray Crystallography," Vol. I, Kynoch Press, Birmingham, England, 1965, p 99.

(13) Computer programs used were Prewitt's absorption correction program ACACA, the least-squares program SFLS5, the Fourier program FOUR, a modification of a program written by C. J. Fritchie, Jr., and various local programs.

(14) L. J. Guggenberger, *Inorg. Chem.*, 7, 2260 (1968).

(15) H. P. Hanson, F. Herman, J. D. Lea, and S. Skillman, *Acta Crystallogr.*, 17, 1050 (1964).

(16) D. H. Templeton, "International Tables for X-ray Crystallography," Vol. III, Kynoch Press, Birmingham, England, 1962, p 216.

This structure refinement is a good example of many of the features that can complicate a crystal structure analysis. Although this problem is not very amenable to the usual X-ray analysis, we feel we have without a doubt established the overall geometry around the Ta atom, which is what we set out to do. Because of the inherent norigidity of the diphosphine ligands we cannot say much in detail about their conformations at any instant in time. There is not much solace in knowing that other similar dimethyldiphosphinoethane structures are similarly disordered in the diphosphine ligand.[27,32]

The final positional and thermal parameters are given in Table I; distances and angles are given in Table II. All atoms in the model are included in Table I for purposes of documentation. A list of observed and calculated structure factors is available.[17]

Nmr Data. Nmr samples were prepared in a nitrogen atmosphere (Vacuum Atmospheres Dri Lab; less than 2 ppm O_2) using deoxygenated solvents. Variable temperature ^1H nmr spectra were recorded in the continuous wave and Fourier modes using a Bruker HFX 90 and in the continuous wave mode using a Varian HR 220 spectrometer. The ^{31}P spectra were recorded in both the continuous wave and Fourier modes at 36.43 MHz with and without ^1H noise decoupling using the Bruker spectrometer. The ^{31}P samples were run in 10-mm tubes with 3-mm coaxial capillaries containing hexafluorobenzene or 1,2-dibromotetrafluoroethane for field-frequency stabilization.

Temperatures for the spectra taken on the HR-220 were measured either by observing the chemical shift separation in methanol or ethylene glycol samples run before and after each trace or by means of a thermometer which fits the spinning nmr tube. For the HFX-90, temperatures were measured by means of a copper–constantan thermocouple located just beneath the sample tube; this thermocouple was calibrated using a similar thermocouple held coaxially in the spinning sample tube partially filled with solvent.

A Digilab FTS/NMR-3 data system and pulser were used to obtain the Fourier mode spectra on the HFX-90. The nmr line shape calculations were carried out using the density matrix method of Kaplan[18] and Alexander.[19] Details concerning the line shape calculations are given elsewhere.[3]

Structure Description

The molecular structure observed is obscured somewhat by the extensive disorder involving the diphosphine, carbonyl, and hydride ligands. We will first describe a physical picture for the disorder which will clarify how we arrive at the geometry for a given molecule as well as some of the refinement details. The disordered model of the diphosphine ligands is shown in Figures 1a and 1b. Physically, the model is consistent with the diphosphine ligands assuming either the solid or dashed configurations in Figure 1 for one of the diphosphine ligands. The solid and dashed configurations for a given diphosphine are related by a simple "flipping" of the ligand, a slight clockwise rotation about one Ta–P direction, and counterclockwise rotation about the other. A center of symmetry at the Ta atom generates the other two configurations to complete the picture of the "average" diphosphine structure observed by X-rays. A side view of the "average" structure is shown in Figure 1b.

The "average" carbonyl and hydride geometry is a superposition of the four configurations shown in Figure 2. This puts two axial carbonyls up and two down with one on either side of those in off-axial positions. The plane of Figure 2 is the vertical plane between the two diphosphines, the idealized molecular mirror plane. The 2:1 ratio of axial to off-axial carbonyl positions explains why the centers of the very elongated CO's were above and below the Ta atom. The carbonyl in the off-axial position is sterically influenced by the hydride hydrogen atom which is also in this plane.

Strictly speaking, the X-ray structure only gives evidence for the average structure; however, the diphosphine and carbonyl disordering must be coupled, and sorting out this coupling enables us to arrive at the actual molecular structure. We believe the diphosphine ligands in a given mole-

(17) See paragraph at end of paper regarding supplementary material.

(18) J. I. Kaplan, *J. Chem. Phys.*, 28, 278 (1958); 29, 462 (1958).

(19) S. Alexander, *J. Chem. Phys.*, 37, 967, 974 (1962); 38, 1787 (1963); 40, 2741 (1964).

Table I. Final Parameters for $TaH(CO)_2[(CH_3)_2PCH_2CH_2P(CH_3)_2]_2$[a]

Atom	x	y	z	B, Å²
Ta	0	0	0	b
P(1)	0.0903 (13)	−0.0211 (7)	0.2282 (10)	7.6 (2)
P(2)	0.2661 (13)	0.1281 (7)	0.1336 (10)	8.1 (2)
C(1)	−0.0448 (91)	0.0160 (45)	0.2880 (68)	7.9 (16)
C(2)	0.1397 (116)	−0.1652 (63)	0.2701 (89)	12.5 (25)
C(3)	0.3110 (103)	0.0368 (56)	0.3578 (79)	9.5 (19)
C(4)	0.3228 (106)	0.1402 (60)	0.3094 (80)	10.5 (21)
C(5)	0.2319 (63)	0.2703 (37)	0.0961 (49)	5.0 (11)
C(6)	0.4957 (142)	0.0835 (91)	0.2110 (111)	16.3 (34)
C(7)[c]	0.1963	−0.1212	0.0392	9.1
C(8)	−0.1364	0.1271	−0.0525	13.8
O(1)	0.3014 (67)	−0.1861 (37)	0.0602 (48)	9.1 (12)
O(2)	−0.2202 (173)	0.2052 (98)	−0.0848 (130)	13.8 (40)
C(1)'[d]	0.1886	−0.1399	0.3305	
C(2)'	−0.1166	0.0060	0.2234	
C(3)'	0.2451	0.0808	0.3458	
C(4)'	0.3812	0.1012	0.3201	
C(5)'	0.4718	0.1100	0.1398	
C(6)'	0.2288	0.2618	0.1624	
C(8)'	0.1941	−0.0781	0.0214	
O(2)'	0.3134	−0.1260	0.0346	

[a] The standard deviations of the parameters varied are given in parentheses. [b] The Ta temperature factor is of the form $\exp[-(h^2\beta_{11} + k^2\beta_{22} + l^2\beta_{33} + 2hk\beta_{12} + 2hl\beta_{13} + 2kl\beta_{23})]$ with $\beta_{11} = 0.0301$ (6), $\beta_{22} = 0.0154$ (2), $\beta_{33} = 0.0136$ (3), $\beta_{12} = 0.0114$ (3), $\beta_{13} = -0.0017$ (3), and $\beta_{23} = -0.0059$ (2). [c] C(7) and C(8) were positioned from the corresponding carbonyl oxygen atoms (see text). [d] The primed atoms are disordered positions related to the unprimed positions and identified as the primed positions in Figure 1a (see text); temperature factors of the corresponding unprimed atoms were used.

Table II. Selected Interatomic Distances and Angles in $Ta(H)(CO)_2[(CH_3)_2PCH_2CH_2P(CH_3)_2]_2$[a]

	Interatomic distances, Å		Interatomic angles, deg
Ta–P(1)	2.497 (12)	P(1)–Ta–P(2)	75.8 (3)
Ta–P(2)	2.530 (9)	P(1)–Ta–P(2)'	104.2 (3)
	2.514 (16)		
		C(7)–Ta–C(8)	163 (3)
Ta–C(7)	2.15 (5)		
Ta–C(8)	1.87 (12)	C(7)–Ta–P(1)	89.2 (13)
		C(7)–Ta–P(2)	87.8 (11)
P(1)–C(1)	1.82 (10)		
P(1)–C(2)	1.85 (8)	O(2)–Ta–P(1)	101.7 (24)
P(1)–C(3)	1.83 (6)	O(2)–Ta–P(2)	82.5 (21)
P(2)–C(4)	1.96 (11)		
P(2)–C(5)	1.81 (5)	Ta–P(1)–C(1)	126.7 (19)
P(2)–C(6)	1.78 (11)	Ta–P(1)–C(2)	107.0 (27)
	1.84 (3)	Ta–P(1)–C(3)	116.2 (23)
		Ta–P(2)–C(6)	120.7 (31)
P(1)–P(2)	3.09 (2)	Ta–P(2)–C(5)	119.5 (14)
C(3)–C(4)	1.45 (12)	Ta–P(2)–C(4)	108.8 (20)
C(1)–C(2)'	0.69 (10)	C(1)–P(1)–C(2)	103.7 (25)
C(2)–C(1)'	0.69 (10)	C(1)–P(1)–C(3)	99.7 (25)
C(3)–C(3)'	0.75 (12)	C(2)–P(1)–C(3)	100.1 (33)
C(4)–C(4)'	0.67 (12)	C(4)–P(2)–C(5)	96.4 (27)
C(5)–C(6)'	0.86 (16)	C(4)–P(2)–C(6)	87.0 (37)
C(6)–C(5)'	0.86 (16)	C(5)–P(2)–C(6)	114.5 (36)
C(7)–C(8)'	0.58 (14)		
O(1)–O(2)'	0.85 (15)	P(1)–C(3)–C(4)	106.4 (49)
		P(2)–C(4)–C(3)	111.6 (52)

[a] The distances involving primed atoms are distances between positions in the disordered model and hence do not represent true bond distances. The primed carbon atoms in the phosphines are identified by primes in Figure 1a; the distances involving primed carbonyl positions are the C–C and O–O distances between the axial and off-axial carbonyls in the disordered model.

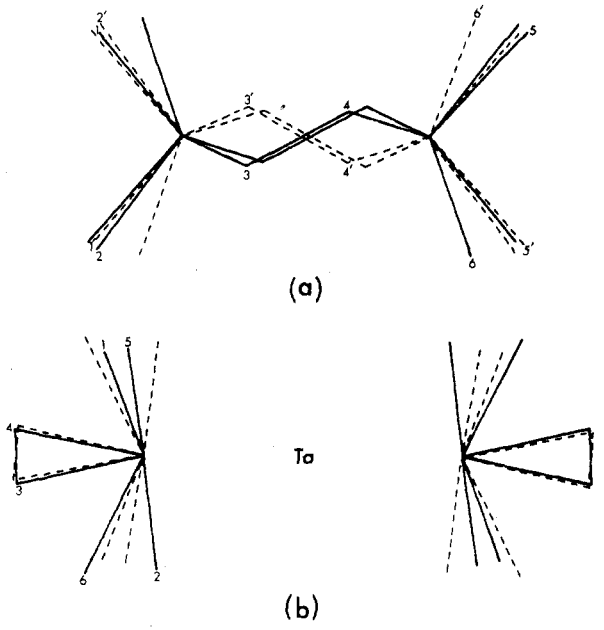

Figure 1. (a) The disordered diphosphine ligands viewed in the PTaP plane normal to the ligand bite [P(1)-P(2) direction]. The solid lines represent the two diphosphine ligands in one conformation (related by $C_i(\bar{1})$); the dotted lines show the corresponding "flipped" conformations. (b) The disordered model viewed in the direction of the ligand bite, a side view of 1a. The solid and dotted lines are the same as in 1a.

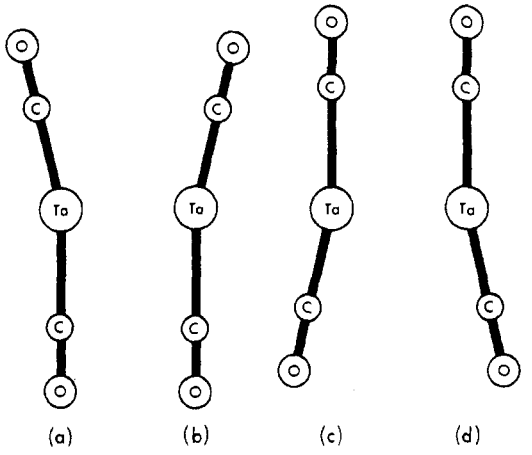

Figure 2. The four configurations which superimpose in the carbonyl disorder.

cule generally maintain an idealized vertical mirror plane as indicated by the two solid configurations in Figure 1. The picture we have then, of one molecule, is shown in Figure 3. The vertical mirror plane is consistent with the bite of the diphosphine ligands and the observed nature of the H-CO disorder in this plane; it also tends to minimize contacts of the C(5)···C(8) and C(1)···H type (Figure 3). For a given TaP_4 geometry the C(8)-O(2) ligand can be displaced toward either the P(1)′-P(2) or P(2)′-P(1) midpoints above the TaP_4 plane or it can assume similar configurations below the TaP_4 plane, in which case the diphosphine ligands would have the dotted line configurations of Figure 1. Looking at this in another way, the "average" molecule is obtained by superimposing the molecule in Figure 3 on the TaP_4 framework in each of the four possible ways; this happens equally and randomly through the crystal.

A single molecule of $TaH(CO)_2[(CH_3)_2PCH_2CH_2P(CH_3)_2]_2$ is not required to have any point symmetry, but it has pseudo

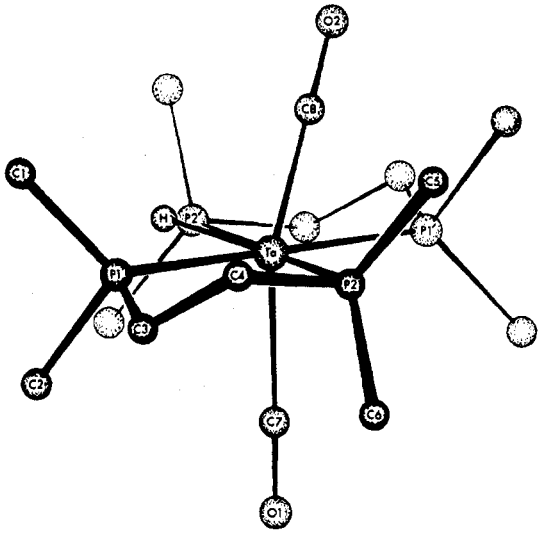

Figure 3. The molecular structure of $TaH(CO)_2[(CH_3)_2PCH_2CH_2P(CH_3)_2]_2$.

$C_s(m)$ symmetry. The molecular mirror plane in Figure 3 contains the Ta, H, C(7), O(1), C(8), and O(2) atoms. The positions of the carbonyl and hydride ligands on the idealized molecular mirror plane result in a large part from the steric constraints of the diphosphine ligands which give a P(1)-P(2) distance of 3.09 (2) Å (in the direction of the ligand bite) and a P(1)-P(2)′ distance of 3.97 (2) Å (normal to the bite direction).

The hydride ligand was not explicitly located, but the disposition of the C(8)-O(2) carbonyl provides a strong indication for the hydride position as shown in Figure 3. The molecular structure is basically a distorted capped octahedron where the least sterically demanding hydride ligand caps the C(8)P(1)P(2)′ face. Similar conformations were found recently for the seven-coordinate complexes $MoBr_2(CO)_3[(C_6H_5)_2PCH_2CH_2P(C_6H_5)_2]$,[20] $MoBr_2(CO)_2[(C_6H_5)_2AsCH_2CH_2As(C_6H_5)_2]_2$[21] (one diarsine monodentate), $MoBr_4[(CH_3)_2C_6H_5P]_3$,[22] and $WBr_3(CO)_4^-$.[23]

The disorder here prohibits the determination of accurate bond lengths, but some comparisons with literature values can be made. We could not find any structures of organometallic complexes with tantalum for direct comparisons. The Ta-P distance of 2.514 (16) Å is in the observed range of Mo-P distances in numerous known structures; the Mo-P distances are usually in the 2.43-2.57 Å range.[9] A W-P value of 2.550 (3) Å was observed in $WCl_4[P(CH_3)_2(C_6H_5)]_2$.[24] The Ta-C(CO) distances also agree with the W-C(CO) distances of 1.95 and 1.99 Å observed in $[(C_2H_5)_4N][WBr_3(CO)_4]$.[23]

The observed diphosphine ligand geometry is similar to that frequently found for diphosphine ligands. The P(1)-Ta-P(2) bite angle of 75.8 (3)° is similar to corresponding P-M-P values as, for example, 76.5 (1)° in $MoBr_2(CO)_3[(C_6H_5)_2PCH_2CH_2P(C_6H_5)_2]$[20] and 75.3 (1)° in $MoCl(C_5H_5)(CO)[(C_6H_5)_2PCH_2CH_2P(C_6H_5)_2]$.[25,26] The angles for

(20) M. G. B. Drew, *J. Chem. Soc., Dalton Trans.*, 1329 (1972).
(21) M. G. B. Drew, *J. Chem. Soc., Dalton Trans.*, 626 (1972).
(22) M. G. B. Drew, J. D. Wilkins, and A. P. Wolters, *J. Chem. Soc., Chem. Commun.*, 1278 (1972).
(23) M. G. B. Drew and A. P. Wolters, *J. Chem. Soc., Chem. Commun.*, 457 (1972).
(24) L. Aslanov, R. Mason, A. G. Wheeler, and P. O. Whimp, *Chem. Commun.*, 30 (1970).
(25) M. A. Bush, A. D. U. Hardy, L. M. Muir, and G. A. Sim, *J. Chem. Soc. A*, 1003 (1971).
(26) J. H. Cross and R. H. Fenn, *J. Chem. Soc. A*, 3020 (1970).

the later transition metal complexes are generally slightly higher, as, for example, 82–85° in $MH(C_{10}H_7)[(CH_3)_2PCH_2CH_2P(CH_3)_2]_2$ (M = Ru, Os),[27] $Rh[(C_6H_5)_2PCH_2CH_2P(C_6H_5)_2]_2(ClO_4)$,[28] and $M(O_2)[(C_6H_5)_2PCH_2CH_2P(C_6H_5)_2]_2(PF_6)$ (M = Rh, Ir);[29] an angle of 88.8 (1)° was found in $NiBr(\pi C_4H_7)[(C_6H_5)_2PCH_2CH_2P(C_6H_5)_2]$.[30] The larger angles result from shorter M–P bond distances. The stereochemistry about the phosphorus atoms is also similar to that found in other diphosphine complexes.[20,25-30] The P–C distances agree with those frequently found when the individual errors are considered; the average P–C distance is 1.84 (3) Å.

The nonhydrogen atom intermolecular contacts were examined and the shortest was 3.26 Å between a methyl carbon atom and a carbonyl oxygen atom. The lack of any strong intermolecular contacts probably contributes to the disorder problem. The individual least-squares planes do not appear to be of any particular significance. The equation for the molecular plane (Ta, P(1), P(2), P(1)′, and P(2)′) relative to the orthogonal coordinate system based on a, b, and c^* is $-0.6667X + 0.7275Y - 0.1622Z = 0$.

The conformational possibilities for the diphosphine ligands are numerous, which is really the crux of the problem here. Four clearly identifiable conformations are shown in I–IV; of course, there is a continuum between these. The

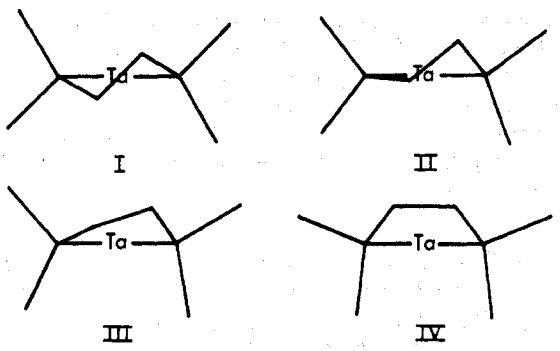

symmetrical I and unsymmetrical II are essentially equivalent in energy.[28,31] The final conformation reported here is close to I; however, in various other refinement models we observed conformations closer to II than reported here. What this probably means is that in addition to the static phenomenon of "flipped" diphosphines there is also a dynamic and/or static disorder introduced by the mixing of I and II type conformations. We feel we can rule out III and IV, or at least relegate them to a low rate of occurrence, because of the observed methyl peaks in our electron density maps; however, they cannot be excluded altogether since their expected distributions in the disordered structure are not very different from I and II. We note incidentally that IV, which is not considered by chemists generally, is really not unreasonable from a steric point of view; it is easy to generate from I and II and readily accessible from III.

Our torsion angles proceeding around the chelate diphosphine ring are 13.3° for Ta–P(1), −41.7° for P(1)–C(3), 49.9° for C(3)–C(4), −40.4° for C(4)–P(2), and 10.4° for P(2)–Ta; these are in the range found in other structures.[28] Another interesting observation is that other dimethylphosphinoethane structures[27,32] are disordered similarly to the present structure. The diphenylphosphinoethane structures[20,25,26,28-30,33] on the other hand tend to be ordered. This is understandable in terms of the influence of ligand steric effects on the packing potentials.

Summarizing with respect to the molecular structure, the data support a distorted capped octahedron as shown in Figure 3. One of the carbonyl ligands is bent away from the axial position because of the steric influence of the hydride hydrogen which is the capping ligand, near the P(1)–C(8)P(2)′ face. The resultant molecular symmetry is essentially $C_s(m)$. The crystal structure is disordered basically because (a) there are several energetically equivalent conformations possible for the diphosphine ligands and (b) there are no strong intermolecular packing potentials to order the packing of the symmetrical diphosphines.

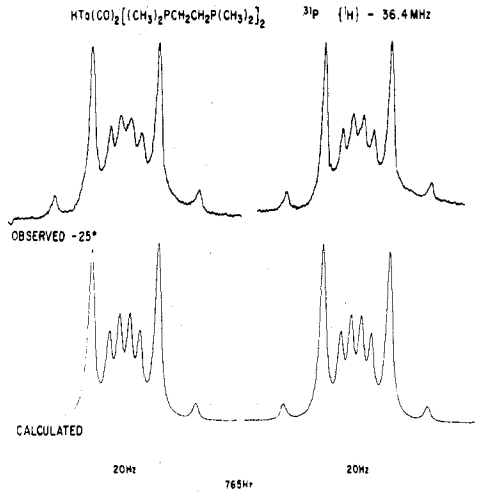

Figure 4. Low-temperature limit proton noise decoupled continuous wave mode 36.43-MHz ^{31}P nmr spectrum of $TaH(CO)_2[(CH_3)_2PCH_2CH_2P(CH_3)_2]_2$. In each half of the spectrum there are two additional low-intensity "wing lines" separated by 107 Hz. The right-hand side of the figure is to high field. The nmr parameters used to obtain the calculated spectrum are given in the text.

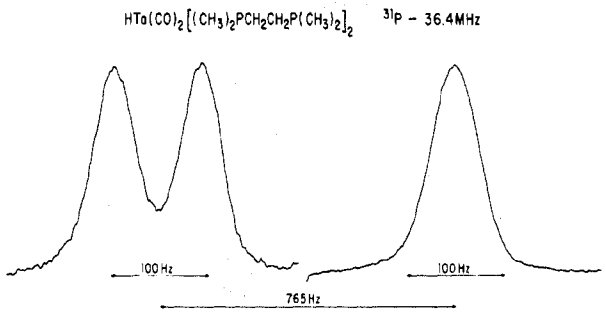

Figure 5. Low-temperature limit continuous wave mode ^{31}P nmr spectrum of $TaH(CO)_2[(CH_3)_2PCH_2CH_2P(CH_3)_2]_2$. The intensities of the two halves of the spectrum are not to scale in the figure (the integrated intensities of the two halves of the spectrum are in a 1:1 ratio). The right-hand side of the figure is to high field.

Nmr Results. The low-temperature limit continuous wave mode proton noise decoupled ^{31}P nmr spectrum of $TaH(CO)_2[(CH_3)_2PCH_2CH_2P(CH_3)_2]_2$ is shown in Figure 4. It consists of an AA′BB′ spectrum approaching the

(27) U. A. Gregory, S. D. Ibekwe, B. T. Kilbourn, and D. R. Russell, *J. Chem. Soc. A*, 1118 (1971).
(28) M. C. Hall, B. T. Kilbourn, and K. A. Taylor, *J. Chem. Soc. A*, 2539 (1970).
(29) J. A. McGinnety, N. C. Payne, and J. A. Ibers, *J. Amer. Chem. Soc.*, 91, 6301 (1969).
(30) M. R. Churchill and T. A. O'Brien, *J. Chem. Soc. A*, 206 (1970).
(31) J. R. Gollogly and C. J. Hawkins, *Inorg. Chem.*, 8, 1168 (1969).
(32) I. W. Nowell, S. Rettig, and J. Trotter, *J. Chem. Soc., Dalton Trans.*, 2381 (1972).
(33) C. G. Pierpont, A. Pucci, and R. Eisenberg, *J. Amer. Chem. Soc.*, 93, 3050 (1971).

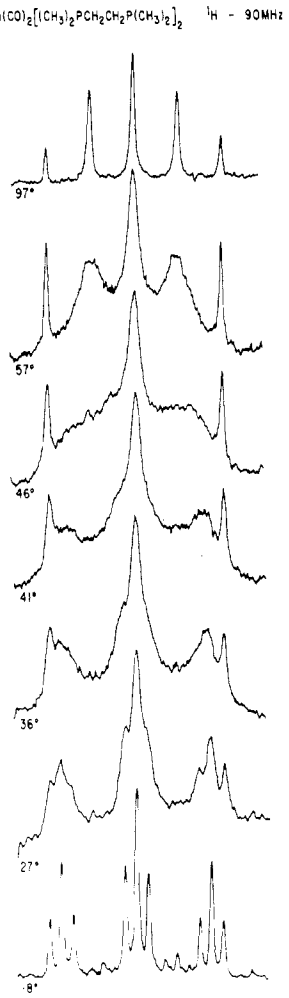

Figure 6. Temperature-dependent continuous wave mode hydride region ^{1}H nmr spectrum of $TaH(CO)_2[(CH_3)_2PCH_2CH_2P(CH_3)_2]_2$ recorded on the HFX 90 spectrometer.

AA′XX′ limit.[34] Not all of the spectrum is shown in Figure 4; for each half there are two additional, almost symmetrically placed, low intensity lines separated by 107 Hz. These lines were not detected in the initial continuous wave mode experiments but were measured subsequently using Fourier techniques. The simulated spectrum shown in the lower half of Figure 4 was calculated using the following parameters: $\delta_A = -32.17$ ppm upfield from 85% H_3PO_4, $\delta_B = -11.12$ ppm ($\delta_B - \delta_A = 766$ Hz at 36.43 MHz), $|J_{AA'} + J_{BB'}| = 52.3$ Hz, $|J_{AA'} - J_{BB'}| = 14.1$ Hz, $|J_{AB} + J_{AB'}| = 16.5$ Hz, and $|J_{AB} - J_{AB'}| = 16.5$ Hz.

The actual coupling constants used to obtain the calculated spectrum shown in Figure 4 were $J_{AA'} = 19.1$ Hz, $J_{BB'} = 33.2$ Hz, $J_{AB} = 16.5$ Hz, and $J_{AB'} = 0$ Hz. When the temperature is raised the spectrum begins to broaden at about 0° and eventually coalesces into a broad line. Because the chemical shift separation between the AA′ and BB′ sites is so large, the spectrum cannot be coalesced into a sharp single line below the boiling point of the fluorine lock material (C_6F_6). Figure 5 shows the low-temperature limit ^{31}P nmr spectrum without noise decoupling. The spectrum is now broad due to unresolved coupling to the ligand protons. The downfield half of the spectrum is split into a doublet due to a large ^{31}P-^{1}H coupling to the single hydride hydrogen ($J_{HP_A} = 89$ Hz).

(34) For a recent review of AA′BB′ and AA′XX′ spectra see H. Gunther, *Angew. Chem., Int. Ed. Engl.*, 11, 861 (1972).

Figure 6 shows the temperature-dependent continuous wave mode hydride region ^{1}H nmr spectra recorded at 90 MHz on the Bruker spectrometer. The low-temperature limit spectrum consists of an essentially first-order triplet of triplets arising from the coupling of the single hydride proton to the AA′ and BB′ phosphorus nuclei. The coupling constants are $J_{HA} = J_{HA'} = 89.25$ Hz and $J_{HB} = J_{HB'} = 14.25$ Hz. As the temperature is raised, the spectrum at first broadens (except for the outer lines) and eventually collapses into a binomial quintet in the high-temperature limit. The high-temperature limit spectrum indicates that the process producing the temperature-dependent nmr line shape effects does not involve a complete dissociation of the $(CH_3)_2PCH_2$-$CH_2P(CH_3)_2$ ligand (an unlikely situation in any case) and that all the H-P coupling constants are averaged. The maintenance of sharp outer lines at all temperatures is characteristic of an intramolecular "mutual" exchange process with all the H-P coupling constants having the same sign (but see the description of the 220-MHz hydride region nmr spectra in the Discussion section below).

The coupling constant obtained from the high-temperature limit spectrum is equal to the average of the low-temperature limit coupling constants. As expected, the Fourier mode spectra are almost identical with the continuous wave mode spectra shown in Figure 6. The chemical shift of the hydride proton is 4.17 ppm upfield from TMS.

The temperature-dependent hydride region ^{1}H nmr spectra recorded at 220 MHz (Figure 7) are quite similar to the 90-MHz spectra shown in Figure 6 except that the spectra are broader at intermediate exchange rates and even the "sharp outer lines" seem to be broadened. This may be due, at least in part, to the poorer resolution achieved using the HR 220 spectrometer.

Discussion

For an $MH(CO)_2P_4$ system with C_s symmetry corresponding to the geometry observed in the X-ray crystal structure of $TaH(CO)_2[(CH_3)_2PCH_2CH_2P(CH_3)_2]_2$, there are eight basic permutational sets[3] including the identity set. In the present case five of these eight sets must be excluded since they consist of permutations which would generate different isomers of the molecule with different nmr parameters (some of these isomers correspond to chemically impossible structures). Because of this restriction, which is a result of the chelate nature of the ligands, there are only two basic types of temperature-dependent line shape behavior which correspond to mutual exchange processes. These are, using the nuclear labeling scheme in Figure 8

Basic set	Equivalent basic set
E (1)(2)(3)(4)	(12)(34)
1 (14)(23)	(13)(24)
2 (1234)	(13)
(1432)	(24)

The nmr line shapes simulated for sets I and II are shown in columns 1 and 2, respectively, of Figure 9. Column 3 shows the line shapes calculated for the linear combination I + II.

It is clear on comparing the observed ^{1}H spectra (Figures 6 and 7) with the spectra simulated for the basic sets I, II, and I + II that the observed spectra cannot be fitted using a mutual exchange model. All simulations using mutual exchange models indicate that the spectrum is symmetric in the low-temperature limit and remains symmetric at all exchange rates. The observed spectra, however, are symmetric at the slow and fast exchange limits but definitely asymmetric at intermediate exchange rates. The sharp outer lines characteristic of a mutual exchange process can be observed at all

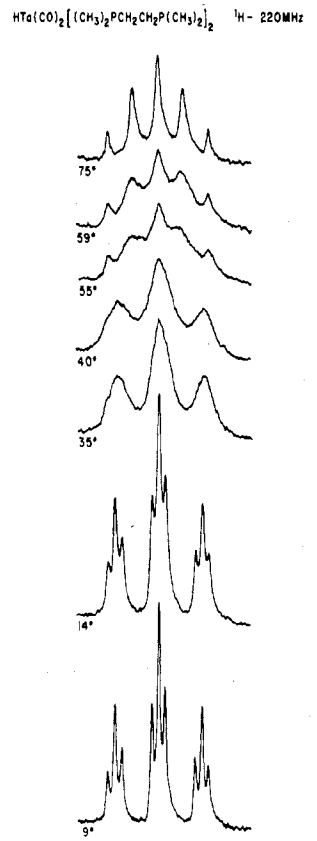

Figure 7. Temperature-dependent continuous wave mode hydride region ^1H nmr spectrum of $TaH(CO)_3[(CH_3)_2PCH_2CH_2P(CH_3)_2]_2$ recorded on the HR 220 spectrometer.

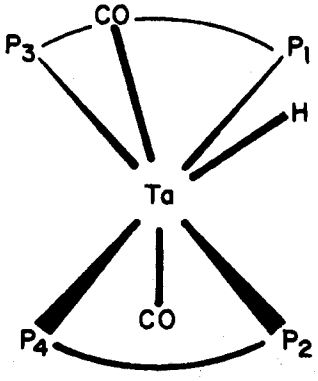

Figure 8. Nuclear labeling scheme used in the permutational analysis.

temperatures in the 90-MHz spectra but not in the 220-MHz spectra. We believe that the most plausible explanation of these differences between observed and simulated spectra is to postulate the presence of a second isomer in solution at low concentrations. The observation that the 220-MHz spectra are broader than the 90-MHz spectra at intermediate exchange rates is consistent with a process in which both chemical shifts and coupling constants are averaged. A possible structure for such a second isomer is shown in Figure 10b. This isomer would also be a reasonable intermediate in the observed exchange process. As the concentration of the second isomer approached zero, the nmr line shapes should approach that simulated for basic set I in Figure 9, and at small concentrations of the second isomer the spectrum would look like a somewhat broadened and asymmetric version of the line shapes simulated using basic set I. There

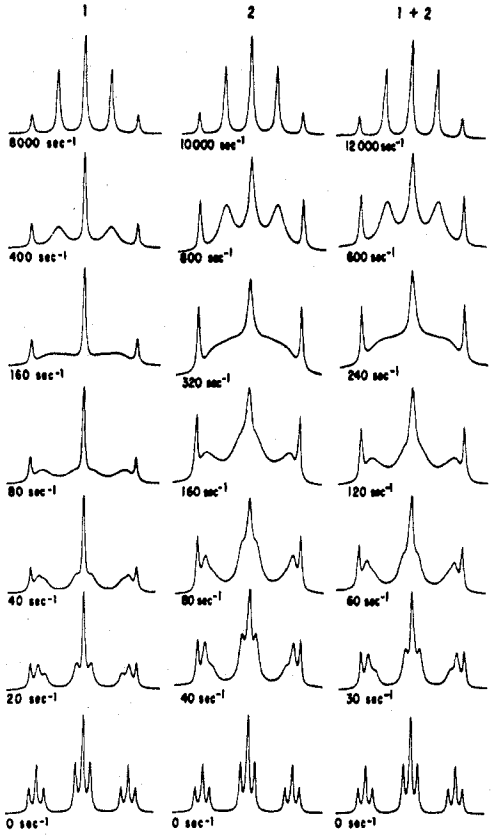

Figure 9. Line shapes simulated for basic sets I and II and the linear combination I + II using a set of high-resolution nmr parameters which fit the observed low-temperature limit proton and proton noise decoupled ^{31}P nmr spectra of $TaH(CO)_2[(CH_3)_2PCH_2CH_2P(CH_3)_2]_2$.

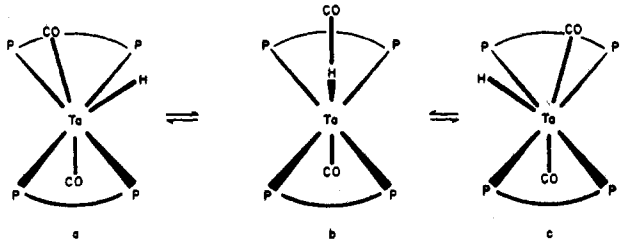

Figure 10. Possible second isomer (b) and exchange mechanism for $TaH(CO)_2[(CH_3)_2PCH_2CH_2P(CH_3)_3]_2$.

is some evidence for a second isomer in solution in the ^{31}P nmr spectra; weak resonances can be observed in the low-temperature limit proton noise decoupled ^{31}P spectrum which do not correspond to the AA'BB' pattern. Some of these resonances do broaden at a lower temperature than the AA'BB' pattern as would be expected for an intermediate with a shorter preexchange lifetime than the most stable isomer.

Although the mechanism outlined above is conceptually very attractive since it exchanged opposite ends of the two chelating ligands simultaneously, it is clear from a comparison of Figures 6 and 9 that there is better agreement between the observed spectra and those simulated for basic set II. Set II corresponds to sequential exchange of the chelate ends and it is difficult to see how this could be achieved in a simple concerted process; dissociation of one end of a $(CH_3)_2PCH_2CH_2P(CH_3)_2$ ligand (arm off mechanism) must be invoked. Even dissociation of a carbonyl ligand would not account for the permutations.

A further process which could occur (possibly with a much

lower barrier than the one we are observing in the proton nmr) involves motion of the hydride ligand through the plane of the phosphorus nuclei rendering the carbonyls equivalent but still maintaining the distinction between the two types of phosphorus. Efforts to observe this process using ^{13}C nmr have been unsuccessful.

In summary, although the distinction is not unambiguous, the results tend to favor permutational set II with an exchange intermediate of sufficient concentration to account for the difference between the 90- and 220-MHz spectra. Since it appears that dissociation of one end of a chelate ligand is required for a mechanism consistent with set II, it is possible that the intermediate observed is an "arm off" species.

Acknowledgment. We would like to thank Mr. G. Watunya and Mr. L. J. Rizzardi for obtaining some of the nmr spectra.

Registry No. $TaH(CO)_2[(CH_3)_2PCH_2CH_2P(CH_3)_2]_2$, 50600-13-0.

Supplementary Material Available. A listing of structure factor amplitudes will appear following these pages in the microfilm edition of this volume of the journal. Photocopies of the supplementary material from this paper only or microfiche (105 × 148 mm, 24× reduction, negatives) containing all of the supplementary material for the papers in this issue may be obtained from the Journals Department, American Chemical Society, 1155 16th St., N.W., Washington, D. C. 20036. Remit check or money order for $3.00 for photocopy or $2.00 for microfiche, referring to code number INORG-74-1025.

Contribution from the Department of Inorganic Chemistry, The University of Sydney, N. S. W. 2006, Australia

Evidence for an Intramolecular C-H···N Hydrogen Bond in (*E*)-5-Methylpyridine-2-carboxaldehyde-2′-pyridylhydrazonetetracarbonylmolybdenum(0) from Its Crystal Structure and Proton Magnetic Resonance Spectrum

R. St. L. BRUCE, M. K. COOPER,* H. C. FREEMAN, and B. G. McGRATH

Received July 13, 1973 AIC30532N

The crystal structure of (*E*)-5-methylpyridine-2-carboxaldehyde-2′-pyridylhydrazonetetracarbonylmolybdenum(0), [Mo(CO)$_4$-(*E*)-5-Me(paphy) = $C_{16}H_{12}MoN_4O_4$], has been determined from three-dimensional X-ray data collected by counter methods. The compound crystallizes in space group $P2_1/c$ with $a = 8.326$ (8), $b = 11.916$ (12), $c = 18.056$ (18) Å, $\beta = 93.15$ (10)°, and $Z = 4$. The structure has been refined by full-matrix least-squares techniques to a residual $R = 0.088$ for 1336 independent nonzero reflections. The organic ligand is bidentate. The resulting chelate ring is planar within the limits of precision of the analysis. The octahedral coordination geometry of the metal is slightly distorted. The mean of the M–C bond lengths is 1.99 (2) Å, the Mo–N bond lengths are 2.26 (1) and 2.27 (1) Å, and the N–Mo–N angle is 72.8 (4)°. A short intramolecular contact (C···N = 2.85 (2) Å) is interpreted as a C–H···N hydrogen bond. Proton magnetic resonance studies show that the short C–H···N contact persists in solution and that it therefore cannot be attributed to crystal packing forces.

Introduction

Complexes of molybdenum(0) with the ligands paphy (pyridine-2-carboxaldehyde-2′-pyridylhydrazone), 5-Me(paphy), 5′-Me(paphy), and 5,5′-Me$_2$paphy exist as pairs of linkage isomers[1,2] in which the ligand adopts the syn or anti configuration about the carbon–nitrogen double bond. These are bidentate chelate compounds in which the metal is bound to the imine nitrogen and one of the pyridyl nitrogens (Figure 1). Analogous pairs of chromium(0) and tungsten(0) complexes have also been prepared.[2]

We now report a crystal structure analysis of the linkage isomer in which the ligand 5-Me(paphy) is coordinated to molybdenum(0) in the anti or *E* configuration about the carbon–nitrogen double bond, the methyl group ensuring unambiguous identification of the pyridyl ring bound to the metal. The analysis was carried out to confirm the correctness of the structure of the parent complex Mo(CO)$_4$-(*E*)-paphy as deduced from the infrared and nmr spectra[1] and to investigate the orientation of the unbound pyridyl ring with respect to the chelating portion of the ligand.

Experimental Section

5-Methylpyridine-2-carboxaldehyde-2′-pyridylhydrazone was prepared by the method of Lions and Martin,[3] the intermediate 5-methylpyridine-2-carboxaldehyde being made according to Ginsburg and Wilson.[4] The hydrazone was recrystallized from aqueous ethanol. *Anal.* Calcd for $C_{12}H_{12}N_4$: C, 67.9; H, 5.7; N, 26.4. Found: C, 67.6; H, 5.6; N, 26.3.

Mo(CO)$_4$-(*E*)-5-Me(paphy) was prepared by the reaction of 5-Me(paphy) and the chloropentacarbonylmolybdate(0) anion[5] at room temperature under a nitrogen atmosphere. Tetraethylammonium chloropentacarbonylmolybdate(0) (1.0 g) was added to a diglyme solution (40 ml) of the ligand (0.5 g). The reaction mixture was stirred for 30 min and filtered to remove the precipitate of tetraethylammonium chloride. Crystallization was induced by the addition of water. After filtering, the complex was washed with ethanol and diisopropyl ether and then stirred with the same solvent for 20 min to remove any molybdenum hexacarbonyl formed as a by-product. The crystals were washed with fresh diisopropyl ether, dried, and stored under nitrogen in the dark. *Anal.* Calcd for $C_{16}H_{12}MoN_4O_4$: Mo, 22.8; C, 45.7; H, 2.9; N, 13.3. Found: Mo, 23.0; C, 45.7; H, 3.2; N, 13.2.

Crystal Data. Mo(CO)$_4$-(*E*)-5-Me(paphy) forms small red crystals stable in air and to X-rays at least for the time necessary for data collection. The unit cell is monoclinic with $a = 8.326$ (8), $b = 11.916$ (12), $c = 18.056$ (18) Å, $\beta = 93.15$ (10)°, $U = 1789$ (3) Å^3, $d_m = 1.59$ (2) g cm^{-3} (by flotation in an aqueous solution of potassium iodide), and $d_x = 1.56$ (3) g cm^{-3} for $C_{16}H_{12}MoN_4O_4$, $Z = 4$, with mol wt 420.3. The space group is $P2_1/c$ (No. 14) from systematic absences of reflections ($0k0$ absent for $k = 2n + 1$, $h0l$ absent for $l =$

(1) R. St. L. Bruce, M. K. Cooper, and B. G. McGrath, *Chem. Commun.*, 69 (1970).
(2) M. K. Cooper and B. G. McGrath, unpublished work.
(3) F. Lions and K. V. Martin, *J. Amer. Chem. Soc.*, **80**, 3858 (1958).
(4) S. Ginsburg and I. B. Wilson, *J. Amer. Chem. Soc.*, 79, 481 (1957).
(5) E. W. Abel, I. S. Butler, and I. G. Reid, *J. Chem. Soc.*, 2068 (1963).